Supplementary information

Contrasting patterns of change in snow line altitude across five Himalayan catchments

Orie Sasaki[1], Evan S. Miles[2], Francesca Pellicciotti[2], Akiko Sakai[1], Koji Fujita[1]

[1]Graduate School of Environmental Studies, Nagoya University, Nagoya, 484－8601, Japan
[2]Swiss Federal Institute for Forest, Snow, and Landscape Research WSL, Birmensdorf, CH-8903, Switzerland

Correspondence to: Orie Sasaki (sasaki.o.ab@m.titech.ac.jp)

Content:

1. Supplementary Figures

- **Figure S1: Monthly total precipitation and mean air temperature for the five target regions**
- **Figure S2: Schematic diagram of the snowline detection algorithm**
- **Figure S3: Comparison of cumulative frequency of SLAs**
- **Figure S4: Comparison of detected SLA among three satellites**
- **Figure S5: Snowlines derived from automatic and manual detections.**
- **Figure S6: Comparison of detected SLAs from this study and standard detection method using MODIS**

2. Supplementary Tables

- **Table S1: Results of the multiple regression analysis for the 60-month moving average**

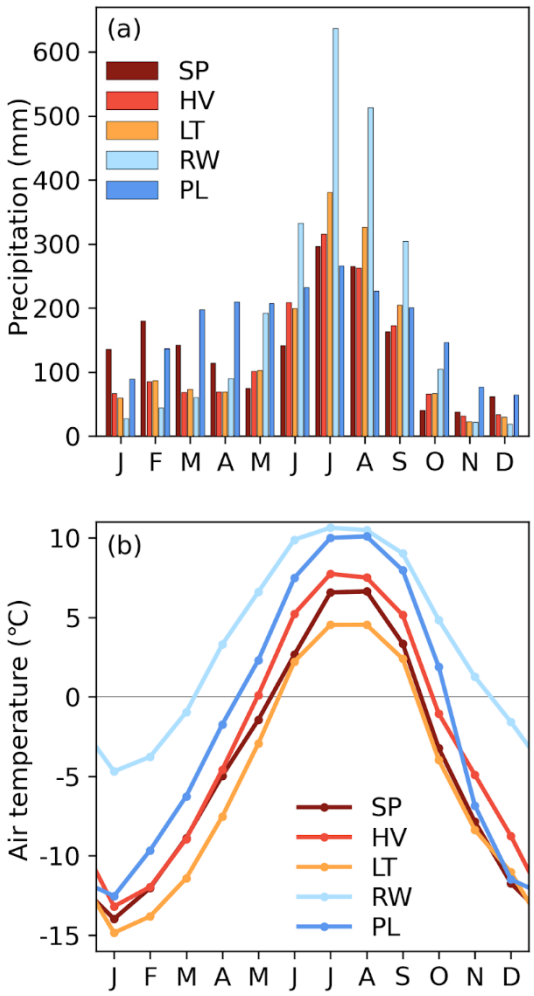

Figure S1: (a) Monthly total precipitation and (b) mean air temperature obtained from the ERA5 reanalysis climate data (Hersbach et al., 2020). The data were averaged for the period from 1999 to 2019 at the grid that includes most of the target catchment without any corrections. Catchment abbreviations denote SP: Satopanth, HV: Hidden Valley, LT: Langtang Valley, RW: Rolwaling Valley, and PL: Parlung, respectively.

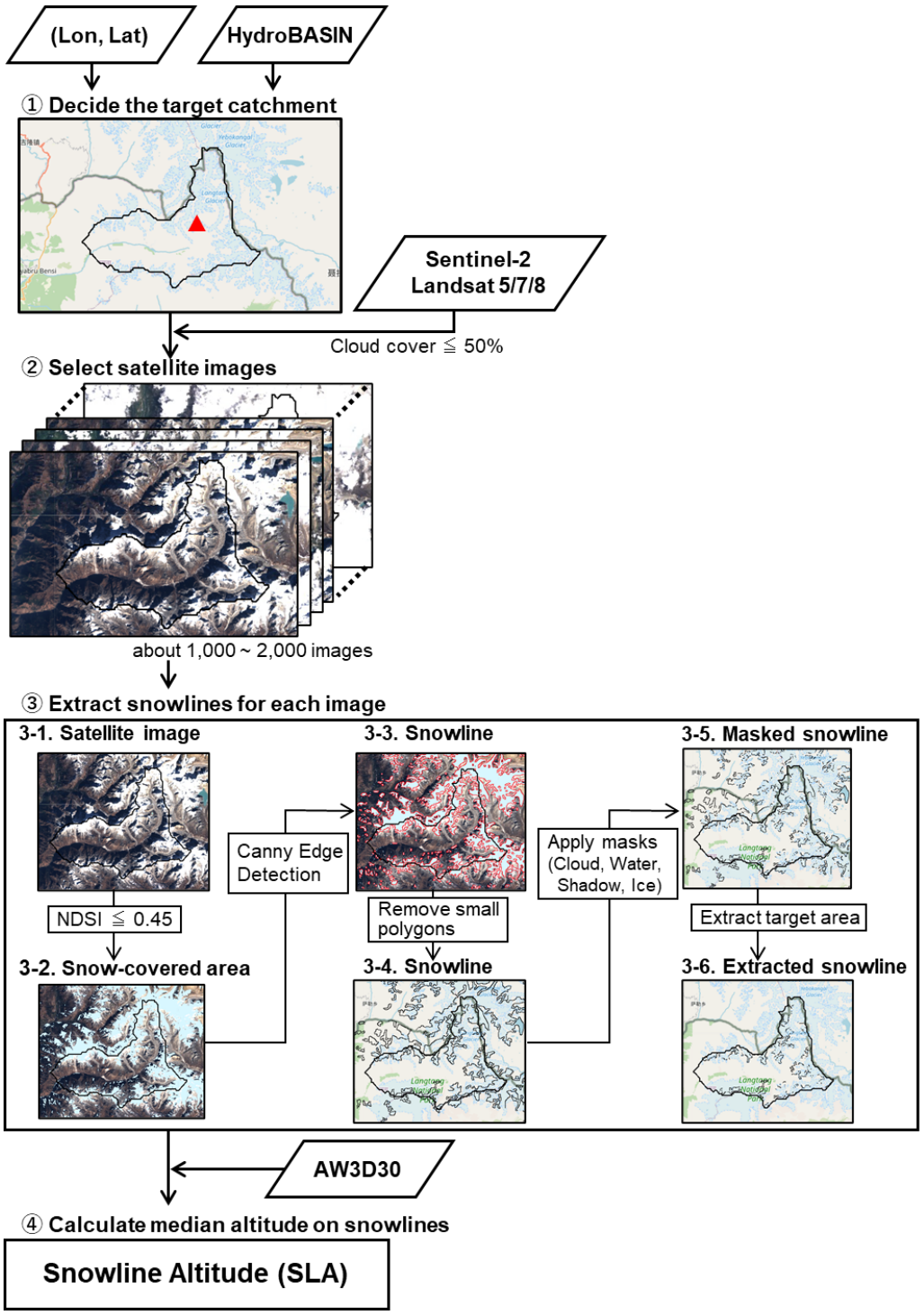

Figure S2: Schematic diagram of the snowline detection algorithm with a sample image obtained from Landsat 8

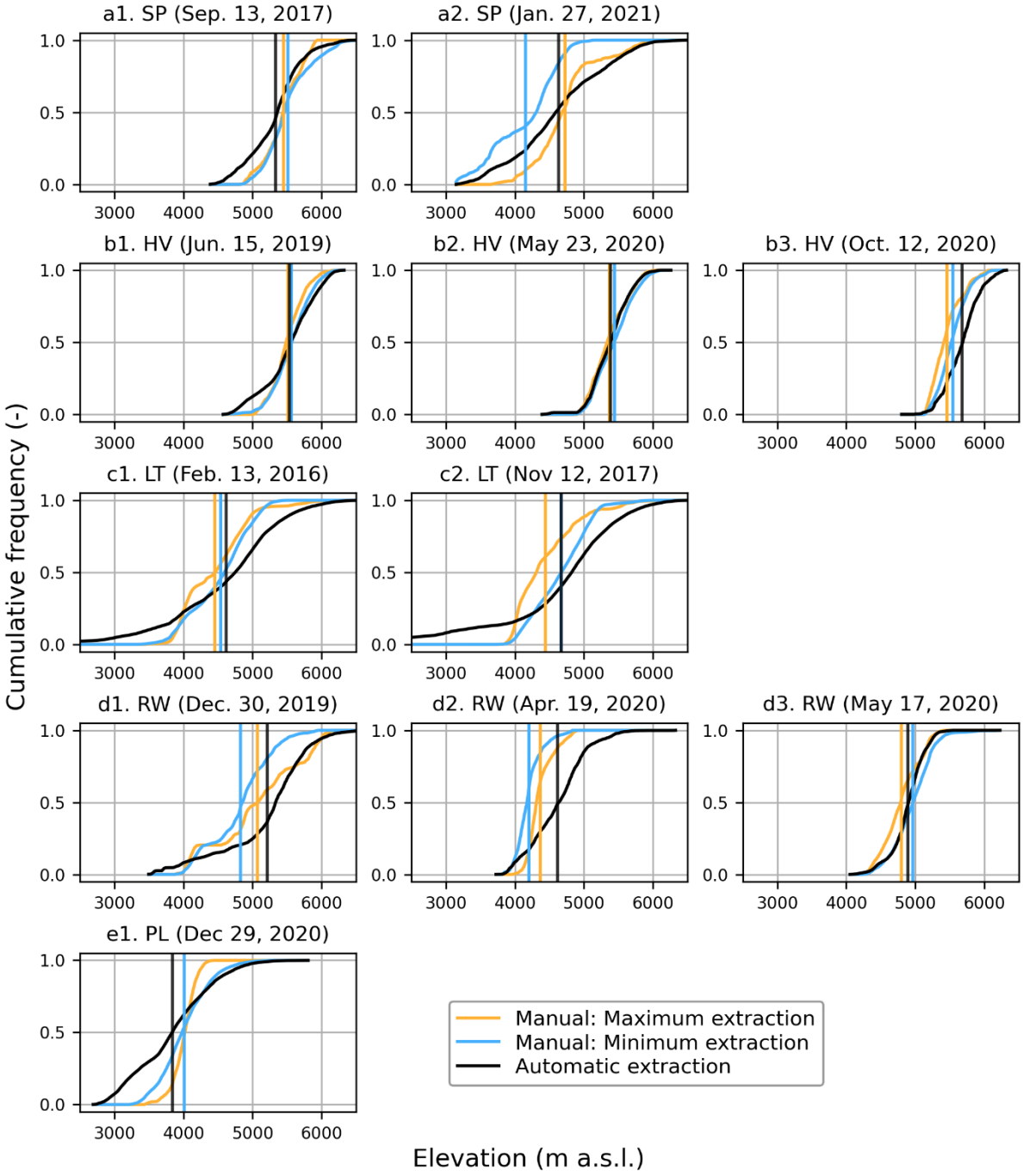

Figure S3: Comparison of cumulative frequency of SLA between the automatically detected snowlines and the manually delineated ones. a1-2, b1-3, c1-2, d1-4, and e1 show the comparison in Satopanth (SP), Hidden Valley (HV), Langtang (LT), Rolwaling (RW), and Parlung (PL), respectively.

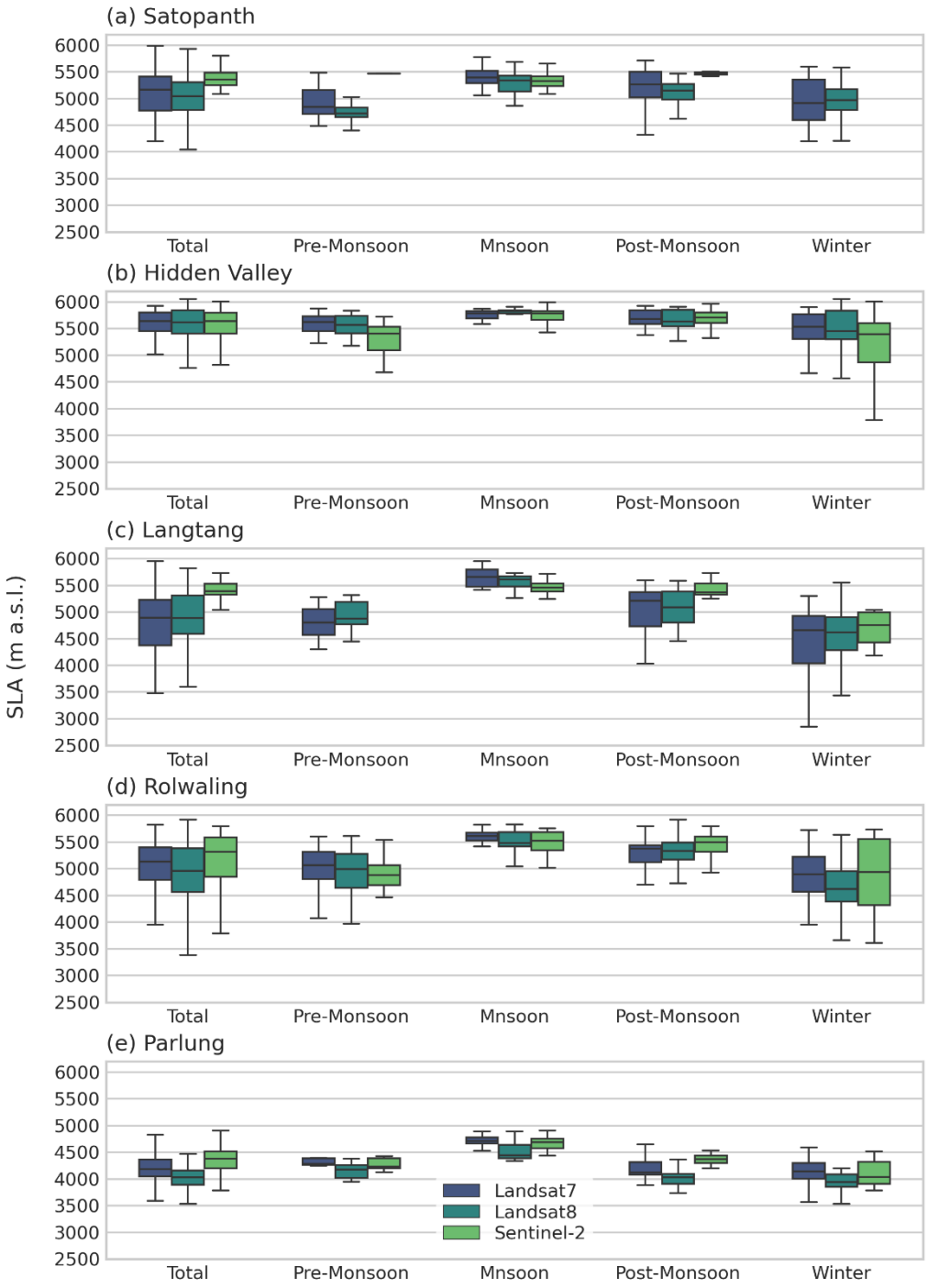

Figure S4: Comparison of cumulative frequency of SLA between the automatically detected snowlines and the manually delineated ones.

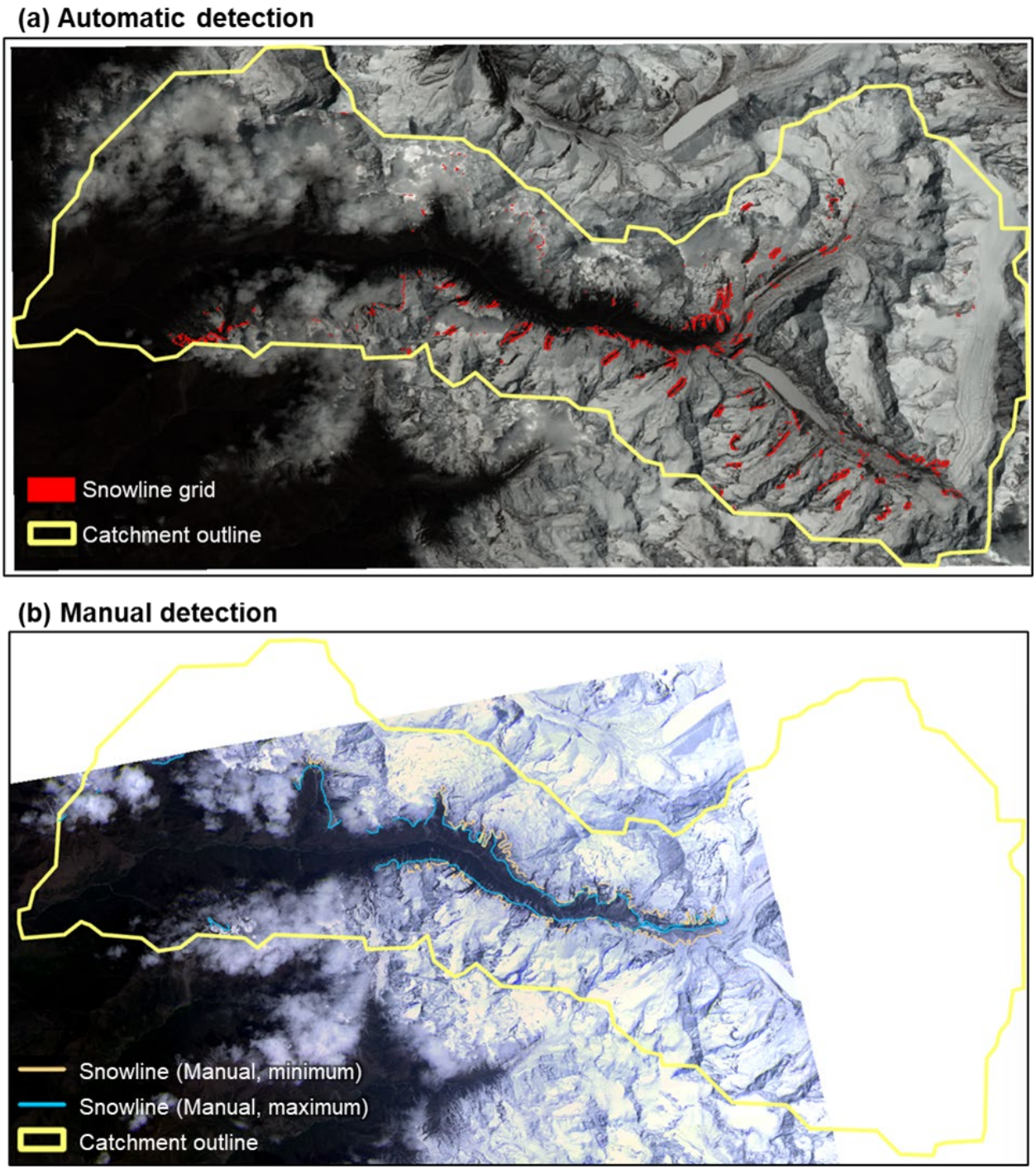

Figure S5: Snowlines derived from (a) automatic detection and (b) manual detection. The background images are the satellite images used for snowline detection: (a) Landsat 8 on April 20, 2020, and (b) PlanetScope on April 19, 2019.

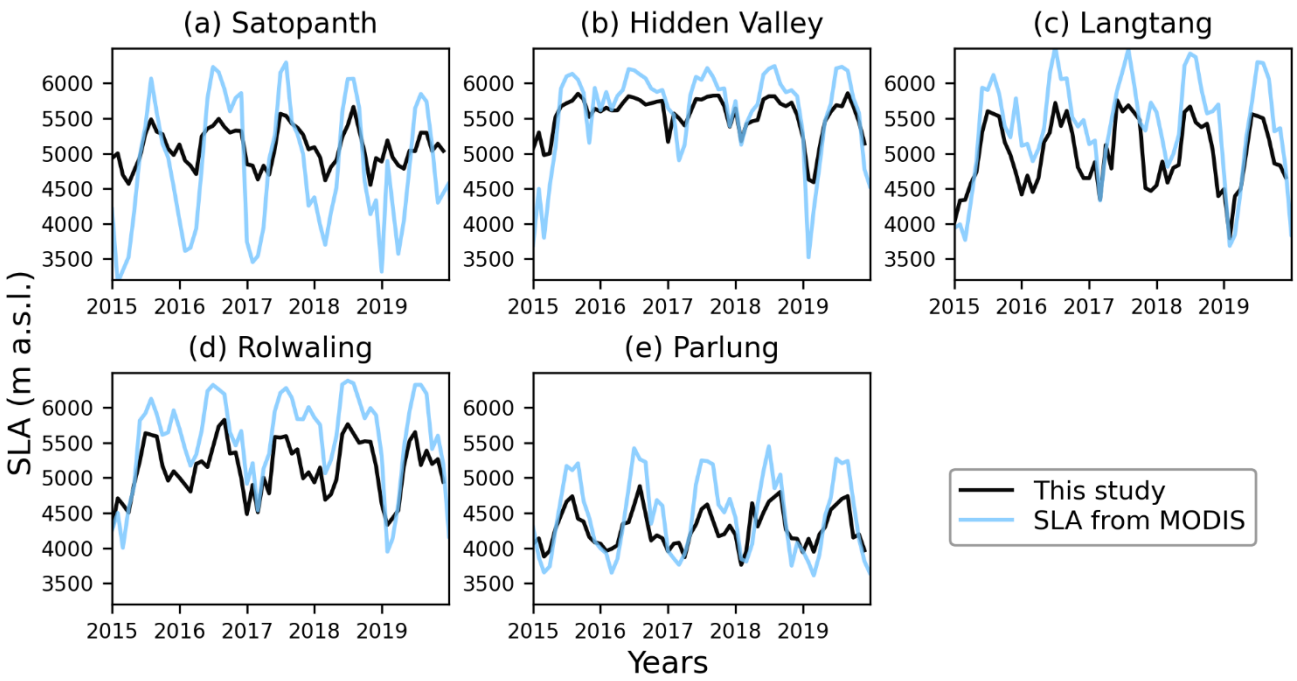

Figure S6: Comparison of detected SLAs from this study and standard detection method using MODIS.

Table S1: Results of the multiple regression analysis using 60-month moving averages of climate data and SLA. Influential factors (p-value < 0.05 and |t-value| > 2.0) are shown in bold. A positive or negative t-value indicates a contribution to the increase or decrease of SLA, respectively.

		Coefficient	Standard error	t-value	p-value
Satopanth	Air temperature	**89.9**	**10.38**	**8.66**	**<0.001**
	Precipitation	**−1.39**	**0.47**	**−2.96**	**0.003**
	Solar radiation	−2.48	1.54	−1.61	0.108
Hidden Valley	Air temperature	**114.54**	**20.39**	**5.62**	**<0.001**
	Precipitation	**8.19**	**0.99**	**8.29**	**<0.001**
	Solar radiation	**24.83**	**5.42**	**4.58**	**<0.001**
Langtang	Air temperature	**123.29**	**16.59**	**7.43**	**<0.001**
	Precipitation	**7.94**	**0.85**	**9.37**	**<0.001**
	Solar radiation	2.90	4.92	0.59	0.556
Rolwaling	Air temperature	**224.13**	**6.34**	**35.35**	**<0.001**
	Precipitation	**7.72**	**0.36**	**21.59**	**<0.001**
	Solar radiation	**28.44**	**1.31**	**21.67**	**<0.001**
Parlung	Air temperature	**33.23**	**9.60**	**3.46**	**0.001**
	Precipitation	−0.03	0.27	−0.12	0.905
	Solar radiation	1.34	0.84	1.29	0.114